

UDC 537.312:538.911'956

Doi: 10.31772/2587-6066-2020-21-4-556-564

For citation: Udod L. V., Romanova O. B., Aplesnin S. S., Kretinin V. V. Study of structural properties of bismuth pyrostannate by Raman and IR spectroscopy. *Siberian Journal of Science and Technology*. 2020, Vol. 21, No. 4, P. 556–564. Doi: 10.31772/2587-6066-2020-21-4-556-564

Для цитирования: Исследование структурных свойств пиростанната висмута методом Раман и ИК спектроскопии / Л. В. Удод, О. Б. Романова, С. С. Аплеснин., В. В. Кретинин // Сибирский журнал науки и технологий. 2020. Т. 21, № 4. С. 556–564. Doi: 10.31772/2587-6066-2020-21-4-556-564

STUDY OF STRUCTURAL PROPERTIES OF BISMUTH PYROSTANNATE BY RAMAN AND IR SPECTROSCOPY

L. V. Udod^{1,2*}, O. B. Romanova², S. S. Aplesnin^{1,2}, V. V. Kretinin¹

¹Reshetnev Siberian State University of Science and Technology

31, Krasnoyarskii rabochii prospekt, Krasnoyarsk, 660037, Russian Federation

²Kirensky Institute of Physics, FRC KSC Siberian Branch of the Russian Academy of Sciences

50, Akademgorodok, Krasnoyarsk, 660036, Russian Federation

*E-mail: luba@iph.krasn.ru

*Chromium-substituted bismuth pyrostannates with a pyrochlore structure were synthesized by the solid-phase reaction method. The X-ray structural analysis performed at room temperature showed that the samples $\text{Bi}_2(\text{Sn}_{1-x}\text{Cr}_x)_2\text{O}_7$, $x = 0; 0.05, 0.1$ are single-phase and belong to the *Pc* monoclinic structure. Polymorphic transformations of the synthesized samples were studied by Raman and IR spectroscopy. IR spectra were obtained at the temperature range 110–525 K and frequencies 350–1100 cm^{-1} . Raman spectra were measured at room temperature at frequencies of 100–3000 cm^{-1} . Heterovalent substitution of Sn^{4+} for Cr^{3+} modifies the spectra of pure $\text{Bi}_2\text{Sn}_2\text{O}_7$. The crystal structure of $\text{Bi}_2\text{Sn}_2\text{O}_7$ consists of two oxygen sublattices: SnO_6 and $\text{Bi}_2\text{O}'$. Chromium ions substituted tin ions in the SnO_6 oxygen octahedra, distorting the local structure in the vicinity of bismuth ions. Phonon modes are softening in the vicinity of phase transitions. A shift of the phase boundaries of polymorphic transitions is observed for $\text{Bi}_2(\text{Sn}_{1-x}\text{Cr}_x)_2\text{O}_7$, $x = 0.05, 0.1$. The frequencies of stretching vibration modes were determined from IR and Raman spectra. The substitution of chromium for tin ions resulted in the appearance of two new modes at frequencies of 581 and 822 cm^{-1} in the Raman spectra. The absence of an inversion center in the crystal structure of $\text{Bi}_2(\text{Sn}_{1-x}\text{Cr}_x)_2\text{O}_7$ is confirmed by Raman spectroscopy. IR spectra of chromium-substituted samples consist of complex lines, which decompose into 2 and 3 Lorentzian lines. The softening and broadening of optical absorption modes are associated with the electronic contribution. Impurity states of electrons form polarons.*

Keywords: bismuth pyrostannate, crystal structure, phase transitions, IR spectroscopy, Raman spectroscopy, X-ray structural analysis.

ИССЛЕДОВАНИЕ СТРУКТУРНЫХ СВОЙСТВ ПИРОСТАНАТА ВИСМУТА МЕТОДОМ РАМАН И ИК СПЕКТРОСКОПИИ

Л. В. Удод^{1,2*}, О. Б. Романова², С. С. Аплеснин^{1,2}, В. В. Кретинин¹

¹ Сибирский государственный университет науки и технологий имени академика М. Ф. Решетнева
Российская Федерация, 660037, г. Красноярск, просп. им. газ. «Красноярский рабочий», 31

² Институт физики им. Л. В. Киренского СО РАН – обособленное подразделение ФИЦ КИЦ СО РАН
Российская Федерация, 660036, г. Красноярск, Академгородок, 50, стр. 38

* E-mail: luba@iph.krasn.ru

*Методом твердофазной реакции синтезированы хромзамещенные пиростаннаты висмута со структурой пирохлора. Рентгеноструктурный анализ, выполненный при комнатной температуре, показал, что образцы $\text{Bi}_2(\text{Sn}_{1-x}\text{Cr}_x)_2\text{O}_7$, $x = 0; 0.05, 0.1$ однофазные и принадлежит к моноклинной структуре *Pc*. Полиморфные превращения синтезированных образцов изучались методами Раман и ИК спектроскопии. ИК-спектры получены в температурном диапазоне 110–525 К, интервале частот 350–1100 см^{-1} . Спектры Рамановского рассеяния измерялись при комнатной температуре на частотах 100–3000 см^{-1} . Гетеровалентное замещение Sn^{4+} на Cr^{3+} видоизменяет спектры чистого $\text{Bi}_2\text{Sn}_2\text{O}_7$. Кристаллическая структура $\text{Bi}_2\text{Sn}_2\text{O}_7$ состоит из двух кислородных*

подрешеток: SnO_6 и $\text{Bi}_2\text{O}'$. Ионы хрома замещают ионы олова в кислородных октаэдрах SnO_6 , искажая локальную структуру в окрестности ионов висмута. Вблизи фазовых переходов происходит смягчение фононных мод. Для $\text{Bi}_2(\text{Sn}_{1-x}\text{Cr}_x)_2\text{O}_7$, 0,05, 0,1 наблюдается смещение фазовых границ полиморфных переходов. Из ИК и Раман спектров определены частоты мод валентных колебаний. В Рамановских спектрах замещение ионов олова хромом привело к появлению двух новых мод на частотах 581 и 822 см^{-1} . Отсутствие центра инверсии в кристаллической структуре $\text{Bi}_2(\text{Sn}_{1-x}\text{Cr}_x)_2\text{O}_7$ подтверждается Раман спектроскопией. ИК спектры хромзамещенных образцов состоят из сложных линий, которые разлагаются на 2 и 3 линии Лоренцевой формы. Смягчение и уширение спектров поглощения связывается с электронным вкладом. Примесные состояния электронов образуют полярны.

Ключевые слова: пироостаннат висмута, кристаллическая структура, фазовые переходы, ИК спектроскопия, Раман спектроскопия, рентгеноструктурный анализ.

Introduction. Bismuth pyrostannate $\text{Bi}_2\text{Sn}_2\text{O}_7$ belongs to the pyrochlore family, which is interesting for its physical properties. These compounds exhibit well-known structural phase transitions of the displacement type in oxygen-octahedral structures, which are usually accompanied by sharp changes in dielectric, mechanical, optical, and other properties.

Three structural modifications were found in polymorphic $\text{Bi}_2\text{Sn}_2\text{O}_7$. Above 900 K, the compound has a cubic structure with small displacements of Bi^{3+} ions from the ideal pyrochlore structure and belongs to the γ -phase. In the temperature range 390–900 K, the β -phase with an orthorhombic structure is realized. At room temperature, $\text{Bi}_2\text{Sn}_2\text{O}_7$ is in a noncentrosymmetric monoclinic structure (α -phase) with space group $P1c1$ [1]. Recently, a low-temperature transition at $T = 140$ K from the monoclinic structure to the lower triclinic system has been discovered [2].

In most cases, the crystal structure of bismuth pyrostannate is cubic with a lattice constant of about 1.0 nm and eight formula units per unit cell. The large A-ion is located in 16d-positions and is eight-fold coordinated by oxygen ions, while the smaller B-ion is located in the octahedral environment of oxygen (16c-positions) and has sixfold coordination. The pyrochlore structure $\text{A}_2\text{B}_2\text{O}_6\text{O}'$ consists of two sublattices: B_2O_6 and $\text{A}_2\text{O}'$. The B_2O_6 sublattice is formed of BO_6 – octahedra connected by an oxygen B – O – B bridge at an angle of 135° into zigzag chains, all B – O bonds are equivalent. The A cation forms the $\text{A}_2\text{O}'$ sublattice from the A – O' chains. Cations A and B in the structure of pyrochlores form a sublattice of tetrahedra connected by corners.

The structure of $\text{Bi}_2\text{Sn}_2\text{O}_7$ is well described by two interpenetrating oxide sublattices. The Sn_2O_6 sublattice consists of SnO_6 octahedra connected by vertices to form hexagonal rings. In the $\text{Bi}_2\text{O}'$ sublattice, the Bi^{3+} cation is tetrahedrally coordinated by O' anions with linear O'–Bi–O' bonds.

It was found that the transitions to the α - and β -phases occur with the rotation of $\text{Bi}_2\text{O}'$ tetrahedra, which displace Bi ions to the top of the SnO_6 oxygen octahedron of the α -phase and the edge in the β -phase [3]. Bismuth ions in their electronic structure have a lone pair of $6s^2$ electrons. These electrons cause mobility of Bi^{3+} and O^{2-} in $\text{Bi}_4\text{O}'$, which leads to distortion of the ideal structure of pyrochlore. Correlated displacements of Bi^{3+} can lead to phase transitions into complex ordered structures, which in turn lead to changes in macroscopic properties.

In the region of structural phase transitions, anomalies on the curves of temperature dependences of dielectric and electrical properties of $\text{Bi}_2\text{Sn}_2\text{O}_7$ are observed [1; 4].

Bismuth pyrostannate is a dielectric. Substitution of tin ions by 3-d elements in $\text{Bi}_2\text{Sn}_2\text{O}_7$ causes distortion of the crystal structure and a shift in phase transitions. For example, heterovalent substitution of Bi^{3+} and Sn^{4+} ions in $\text{Bi}_2\text{Sn}_2\text{O}_7$ leads to a change in the temperature of the $\alpha \rightarrow \beta$ transition [5–7].

In the region of the $\alpha \rightarrow \beta$ structural phase transition, the compound $\text{Bi}_2(\text{Sn}_{1-x}\text{Cr}_x)_2\text{O}_7$, $x = 0.1$ completely changes the conductivity type from hopping (Mott conductivity) to the Poole-Frenkel tunnel emission type. The conductivity of $\text{Bi}_2(\text{Sn}_{1-x}\text{Cr}_x)_2\text{O}_7$, $x = 0.15$ at the $\alpha \rightarrow \beta$ transition is mixed, some of the domains of the compound carry out charge transfer according to the Mott conductivity type, and the other according to the Poole-Frenkel type. The ratio between these phases is approximately 50×50 [5; 8].

An electronic transition with a change in the conductivity type from the hopping to the tunnel emission Poole-Frenkel type at the $\alpha \rightarrow \beta$ structural transition is observed at isovalent substitution of $\text{Bi}_2(\text{Sn}_{0.9}\text{Mn}_{0.1})_2\text{O}_7$.

Substitution of manganese for tin ions changed the type of thermal effects during structural phase transitions from exothermic to endothermic [7]. Anomalies of the dielectric constant are observed in the region of the $\alpha \rightarrow \beta$ transition. For example, the real part of the dielectric constant $\text{Re}(\epsilon)$ $\text{Bi}_2(\text{Sn}_{0.9}\text{Mn}_{0.1})_2\text{O}_7$ has an inflection point at 418 K and a sharp rise above 700 K, the imaginary part $\text{Im}(\epsilon)$ exhibits a maximum at $T = 425$ K and an increase that begins from $T \sim 700$ K [7].

Anomalies of the dielectric constant in the temperature range of phase transitions are also observed in chromium-substituted pyrostannates. In the $\text{Bi}_2(\text{Sn}_{1-x}\text{Cr}_x)_2\text{O}_7$ system, a broad maximum in $\text{Re}(\epsilon)$ and $\text{Im}(\epsilon)$ at about 420 K is observed with their further increase near the $\beta \rightarrow \gamma$ transition [9].

The structural $\alpha \rightarrow \beta$ transition is accompanied by anomalies in the temperature behavior of the magnetic susceptibility. In the compound $\text{Bi}_2(\text{Sn}_{0.95}\text{Mn}_{0.05})_2\text{O}_7$ [10] antiferromagnetic exchange prevails, and in $\text{Bi}_2(\text{Sn}_{1-x}\text{Cr}_x)_2\text{O}_7$ ferromagnetic exchange dominates [5; 11–12].

The absence of an inversion center in bismuth pyrostannate is a prerequisite for the existence of ferroelectric

order at low temperatures. Theoretical calculations carried out from first principles confirm this assumption. In $\text{Bi}_2(\text{Sn}_{0.8}\text{Fe}_{0.2})_2\text{O}_7$ magnetoelectric interaction up to 300 K was found [13–14]. An external electric field leads to deformation of the crystal lattice and to the formation of electric polarization.

The magnetic field-induced electric polarization is an even function of the magnetic field, with the exception of the 140–160 K structural phase transition region, where the linear magnetoelectric effect predominates. The magnetic field-induced electrical polarization decreases with heating. The structural phase $\alpha \rightarrow \beta$ transition and the transition from a noncentrosymmetric to a centrosymmetric structure are accompanied by maxima in the temperature dependence of the dielectric constant and thermoelectric power.

Cationic doping changes the structure of pyrochlore and the basic physical properties of the compounds, since the structural and physical properties are correlated with each other. This group of compounds can be potentially in demand as materials for electrochemical devices, electronic devices of a new generation due to the relatively low synthesis temperatures of doped bismuth pyrostanates and a significant increase in their thermal stability. The possibility of distributing atoms of doping elements over two equivalent crystallographic positions increases the variability of the properties of compounds, due to the different nature of the doping element, affects the defectiveness of the cationic and anionic sublattices, and the transport properties of ions (in particular, mobile oxygen O').

At polymorphic transitions in a wide temperature range, the electric polarization can be controlled by the magnetic field. Multiferroics, which include substituted bismuth pyrostanates, are widely used in electronics and telecommunication technologies. They can be used as polarizers in a wide frequency range from 10^{10} – 10^{15} Hz, for magnetic memory devices and spin electronics, in magnetic random access memory, which combines the speed of semiconductor electronics and non-volatility. Multiferroics serve as the basis for the creation of ME elements of spintronics, in microwave devices as valves, modulators.

Based on the information presented, the purpose of this work is to study the effect of replacing Sn^{4+} ions with Cr^{3+} ions on the structural properties by X-ray diffraction analysis and IR, Raman spectrometry.

Experimental results and discussion. *Synthesis and X-ray structural analysis.* The study of the structural properties by X-ray diffraction analysis, Raman and IR spectroscopy was carried out on polycrystalline samples. Compounds of complex oxide $\text{Bi}_2(\text{Sn}_{1-x}\text{Cr}_x)_2\text{O}_7$, $x = 0; 0.05, \text{ and } 0.1$ were obtained by solid state reaction method according to the following reaction:



A mixture of oxides SnO_2 , Cr_2O_3 and Bi_2O_3 in a stoichiometric ratio was ground for a long time in an agate mortar, pressed into tablets, placed in an oven and kept at a temperature from 973 to 1223 K, the holding time varied from 8 to 24 hours [11; 12].

X-ray structural analysis was performed on the synthesized samples. X-ray powder diffraction patterns of $\text{Bi}_2(\text{Sn}_{1-x}\text{Cr}_x)_2\text{O}_{7-x}$, $x = 0; 0.05, 0.1$ were carried out at room temperature on a Bruker D8 ADVANCE diffractometer using a VANTEC linear detector and $\text{Cu-K}\alpha$ radiation. During the experiment, different sizes of the primary beam slits were used: 0.6 mm in the range of angles $2\Theta = 5$ – 70° and 2 mm in the range of 70 – 120° . The scanning step is 0.016° and remained constant in all areas, the exposure time at each step is 1.5 and 1 s for the ranges 5 – 70° and 70 – 120° , respectively. The standard deviations of the intensities of all points of the X-ray diffraction pattern were calculated, and then the intensities and standard deviations of all points of the high-angle part were multiplied by a normalizing factor of 0.45. All peaks corresponded to the monoclinic cell of the Pc α -phase $\text{Bi}_2\text{Sn}_2\text{O}_7$ [15]. The crystal structure contains 32 Bi^{3+} ions, 32 Sn^{4+} ions, and 112 O^{2-} ions in the independent part of the cell (fig. 1). All Bi^{3+} ions are coordinated by 8 O^{2-} ions and form distorted cubes, while Sn^{4+} ions are coordinated by 6 O^{2-} ions and form octahedra, which are connected by vertices.

The coordinates of all 176 atoms were fixed, since the number of coordinates alone, 528, is comparable to the number of observed reflections. Nevertheless, even the fixed coordinates of the atoms made it possible to correctly describe all the present reflections, and the refinement yielded low uncertainty factors (tab. 1, fig. 2, a).

A linear decrease of the unit cell volume with an increase in the concentration of the substitution ion (fig. 2, b) confirms the single-phase nature of the $\text{Bi}_2(\text{Sn}_{1-x}\text{Cr}_x)_2\text{O}_7$ compositions, since the ionic radius $\text{IR}(\text{Cr}^{3+}, \text{CN}=6) = 0.615 \text{ \AA}$ is less than the radius of the IR ion ($\text{Sn}^{4+}, \text{CN}=6) = 0.69 \text{ \AA}$ [16]. Cr^{3+} ions preferably occupy octahedral positions.

IR spectroscopy. Studies of $\text{Bi}_2(\text{Sn}_{1-x}\text{Cr}_x)_2\text{O}_7$ by IR spectroscopy were performed on a Fourier transform spectrometer Vertex 80 v with a spectral resolution of 1 cm^{-1} in the temperature range 110–525 K, the frequency range 350–1100 cm^{-1} . The studies were carried out on a sample in the form of a tablet with a diameter of 13 mm in a KBr matrix.

The absorption bands of the IR spectra of $\text{Bi}_2\text{Sn}_2\text{O}_7$ in the frequency range of 100–1000 cm^{-1} are usually attributed to the stretching vibrations of the crystal lattice ions. These compounds have seven active IR modes, stretching and bending [17] and concern only vibrations of oxygen atoms occupying two crystallographic positions in the crystal structure of $\text{A}_2\text{B}_2\text{O}_6\text{O}'$.

IR absorption spectra at room temperature in the frequency range 350–1200 cm^{-1} for $\text{Bi}_2(\text{Sn}_{1-x}\text{Cr}_x)_2\text{O}_7$, $x = 0; 0.05$ are shown in fig. 3.

The IR spectrum of $\text{Bi}_2\text{Sn}_2\text{O}_7$ contains 4 main vibration modes: 521, 615, 726 and a broad complex mode in the region at 800 cm^{-1} (tab. 2). The stretching vibration mode $\omega = 521$ is attributed to stretching vibrations of oxygen in the SnO_6 octahedron and splits into two lines at 518 and 525 cm^{-1} . The IR spectra of pyrochlore compounds have very weak absorption bands in the frequency range 800–1100 cm^{-1} , which were identified as an additional complex structural mode of the A–O' long bond

in the A_2O' sublattice. The difference in bond lengths is 20 % between 2.351 Å and 1.961 Å, and the displacement of the O' anion and the A cation within the domain leads to the shortening of one $A - O'$ bond and lengthening of the other [18]. According to this model, the vibrations of the short $A - O'$ bond correspond to phonon modes at about 850 cm^{-1} and vibrations of the long bond at 483 cm^{-1} .

The substitution of tin by chromium ions led to a modification of the IR spectrum, which also contains four distinct groups of lines in the frequency ranges 370–440, 480–560, 580–680, 820–920 cm^{-1} .

All lines of this spectrum are complex and consist of several lines: the frequency range 370–440, 480–560, 580–680 cm^{-1} contains 2 lines, and 820–940 cm^{-1} – 3 lines.

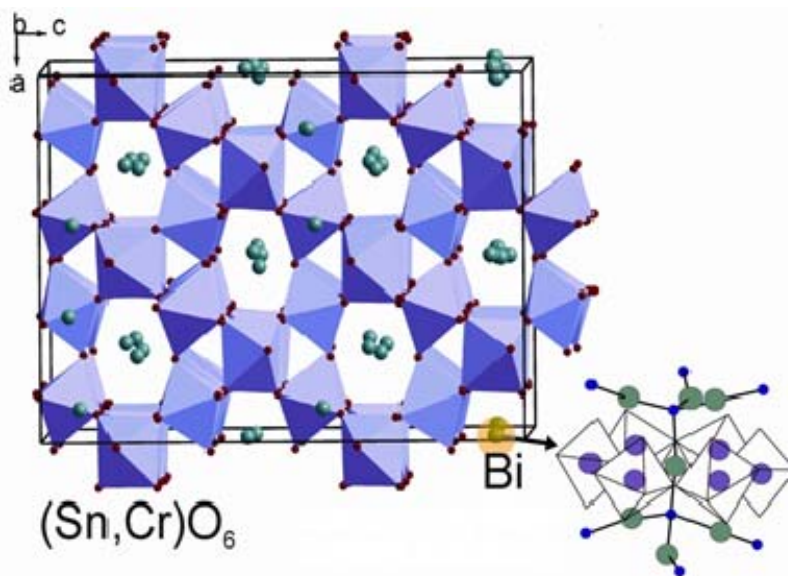


Fig. 1. $\text{Bi}_2(\text{Sn}_{1-x}\text{Cr}_x)_2\text{O}_{7-x}$, $x = 0; 0.05, 0.1$ crystal structure. The BiO_8 fragment is shown separately. There are Sn ions in the center of octahedra. Color code: O atoms are at the vertices of the blue octahedra, O' atoms are dark blue

Рис. 1. Кристаллическая структура $\text{Bi}_2(\text{Sn}_{1-x}\text{Cr}_x)_2\text{O}_{7-x}$, $x = 0; 0.05, 0.1$. Подрешетка BiO_8 выделена отдельно. В центре октаэдров находятся ионы Sn. Атомы O находятся в вершинах голубых октаэдров. Атомы O' – темно голубые

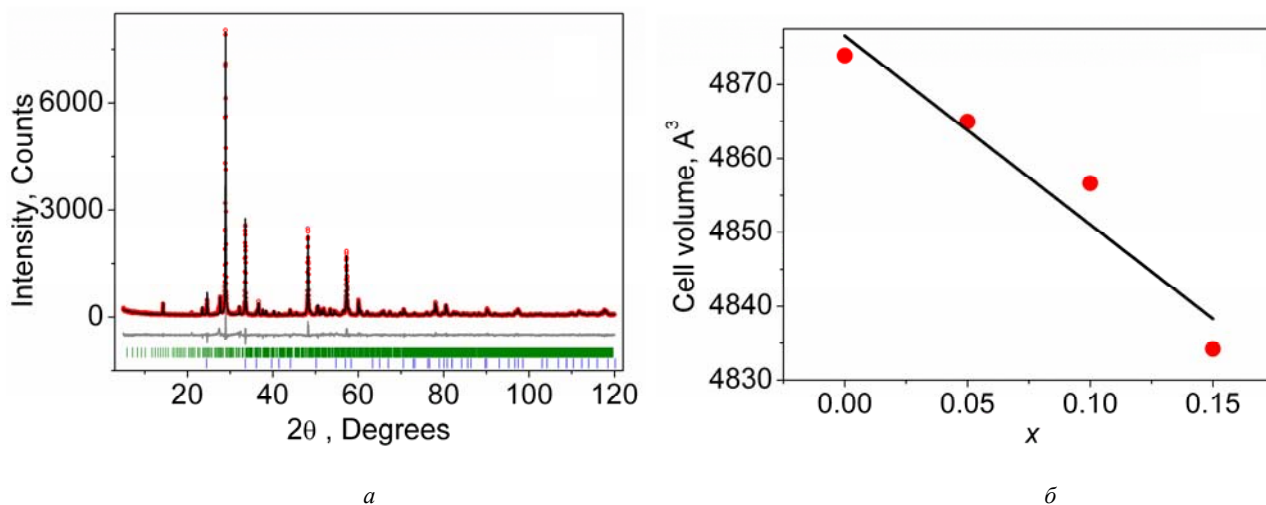


Fig. 2. Difference XRD pattern of $\text{Bi}_2(\text{Sn}_{1-x}\text{Cr}_x)_2\text{O}_7$ (a). Cell parameters of $\text{Bi}_2(\text{Sn}_{1-x}\text{Cr}_x)_2\text{O}_7$ (b)

Рис. 2. Разностная рентгенограмма $\text{Bi}_2(\text{Sn}_{1-x}\text{Cr}_x)_2\text{O}_7$ (a). Параметры ячейки $\text{Bi}_2(\text{Sn}_{1-x}\text{Cr}_x)_2\text{O}_7$ (b)

The main parameters experiments and refinement results of $\text{Bi}_2(\text{Sn}_{1-x}\text{Cr}_x)_2\text{O}_7$

X	0.05	0.1
Space group	Pc	Pc
$a, \text{Å}$	15.0634 (13)	15.075 (1)
$b, \text{Å}$	15.1055 (12)	15.0823 (1)
$c, \text{Å}$	21.381 (2)	21.3589 (13)
$\beta, ^\circ$	89.924 (7)	89.905 (4)
$V, \text{Å}^3$	4865.0 (7)	4856.6 (5)
2θ interval, $^\circ$	5–90	5–90
$R_{\text{wp}}, \%$	13.93	13.62
$R_p, \%$	10.21	10.06
$R_B, \%$	5.08	5.56
χ^2	1.75	1.70

This is agree with the X-ray structural data for $\text{Bi}_2(\text{Sn}_{0.95}\text{Cr}_{0.05})_2\text{O}_7$. The vibration frequency of ions is determined by the symmetry of the crystal lattice.

The frequency range 370–440 cm^{-1} of the IR spectrum of $\text{Bi}_2(\text{Sn}_{0.95}\text{Cr}_{0.05})_2\text{O}_7$ (fig. 3) contains a set of lines with frequencies of 378, 416 cm^{-1} . The mode at a frequency of 382 cm^{-1} is a stretching Bi – O mode of the ideal pyrochlore structure [12]. The 416 cm^{-1} line corresponds to oxygen vibrations in the SnO_6 octahedron.

The next frequency range 490–540 cm^{-1} at room temperature contains two broadened lines with frequencies of 506, 526 cm^{-1} (fig. 3), corresponding to stretching vibrations of the Bi – O' bond in $\text{Bi}_2\text{Sn}_2\text{O}_7$.

In the frequency range 610–640 cm^{-1} , the IR spectrum of $\text{Bi}_2(\text{Sn}_{0.95}\text{Cr}_{0.05})_2\text{O}_7$ at room temperature has a broadened line, which consists of two lines (fig. 3) with frequencies of 618 and 632 cm^{-1} . IR absorption in this frequency range is attributed to stretching vibrations of the Sn – O bond of the oxygen octahedron SnO_6 in the pyrochlore structure [12].

Low-intensity absorption is observed in the high-frequency range 850–920 cm^{-1} . The absorption spectrum has a shoulder at 863 cm^{-1} and a broadened line consisting of 2 lines with frequencies of 878 and 894 cm^{-1} . In the $\text{Bi}_2(\text{Sn}_{0.95}\text{Cr}_{0.05})_2\text{O}_7$ solid solution, the substitution of tin by chromium distorts the local structure in the vicinity of bismuth ions, and the vibrations of the Bi – O' – Cr bonds correspond to these frequencies. In $\text{Bi}_2\text{Sn}_2\text{O}_7$, the lone electron pairs of Bi^{3+} are shortened due to the overlap of Bi 6s electron pairs and d-orbitals of Sn^{4+} . The ionic radii of Sn^{4+} , Cr^{3+} and Bi^{3+} are 0.067, 0.064, 0.120 nm respectively. Chromium ions predominantly occupy octahedral positions; therefore, it can be assumed that chromium replaces tin ions in SnO_6 , distorting the nearest environment.

Almost all vibration frequencies decrease monotonically with increasing temperature, except for the vibration frequency of the Sn-O bond at 630 cm^{-1} . A slight softening of the frequencies at 878 and 894 cm^{-1} upon heating and a decrease in their intensity is observed at a temperature of 330 K. This is possibly due to the electronic contribution to the absorption spectrum. Impurity states of

electrons (holes) form a bound state with phonons – a polaron. At a certain value of the parameter of the electron-phonon interaction, a quasigap is formed in impurity polaron states. With increasing temperature, the chemical potential falls into the forbidden polaron subband and the intensity of thermal transitions decreases at $T = 330$ K.

In the vicinity of a temperature of 260 K, another transition in the absorption intensity was found. IR absorption reaches a maximum at a frequency of 508 cm^{-1} , corresponding to the vibration of a single Bi-O' bond. It is possible that a center of symmetry appears in one of the phases, i.e. a centrosymmetric – noncentrosymmetric phase transition is realized. This assumption is supported by the presence of a maximum dielectric constant at 260 K [11].

Raman spectroscopy. Micro-Raman scattering spectra were measured in backscatter geometry at room temperature through a 50x microscope objective using a Renishaw Via micro-Raman spectrometer equipped with an argon laser (514.5 nm, maximum power 10 MW). The spectral signal was scattered by a 2400 groove/mm diffraction grating on a Peltier-cooled CCD detector with a resolution of 1 cm^{-1} .

The absence of a center of symmetry in the α -phase is also confirmed by Raman scattering spectra. Experimental data of Raman spectroscopy $\text{Bi}_2(\text{Sn}_{1-x}\text{Cr}_x)_2\text{O}_7$, $x = 0, 0.1$ are shown in fig. 4 in the frequency range 100–1000 cm^{-1} at room temperature. The spectrum of $\text{Bi}_2\text{Sn}_2\text{O}_7$ consists of a number of broad bands and is consistent with the spectrum data [19]. The ideal pyrochlore structure $A_2B_2O(1)_6O(2)$ with a space group $Fd\bar{3}m$ has several types of vibrations $\Gamma_R = A_{1g} + E_g + 4F_{2g}$. In this view, the six main Raman modes are active. The spectra shown in fig. 4 have a number of spectral lines that differ from the ideal pyrochlore structure, as a result of a decrease in symmetry (tab. 2).

Bismuth pyrostannate with symmetry $Pc(C_s^2)$ has a larger number of active modes $\Gamma_R = 526A' + 527A''$. In the frequency range 100–200 cm^{-1} for $\text{Bi}_2(\text{Sn}_{1-x}\text{Cr}_x)_2\text{O}_7$, $x = 0$, bending (F_{1u}) O-Bi-O, 148 cm^{-1} and stretching (F_{1u}) Bi- SnO_6 , 188 cm^{-1} vibrations are active [6].

In the intermediate region of the spectrum of $\text{Bi}_2\text{Sn}_2\text{O}_7$, 200–400 cm^{-1} some modes correspond to active vibrations of IR spectroscopy for pyrochlores with low symmetry. The spectral line at 211 cm^{-1} is predominantly described by stretching vibrations (F_{1u}) along the Bi-SnO₆ bond. Vibrations with frequencies of 274, 382 cm^{-1} are defined as stretching (F_{1u}) O-Sn-O and

stretching (F_{1u}) Bi-O. Within this range, there are two modes that correspond to the ideal pyrochlore structure, 225 (F_{2g}) and 248 cm^{-1} (E_g). The mode (F_{2g}) is associated with the shift of oxygen O1 in the SnO₆ polyhedron. Four groups of vibrations are observed in the Raman spectrum of $\text{Bi}_2\text{Sn}_2\text{O}_7$ above 400 cm^{-1} . Vibrations of 535 and 400 cm^{-1} are classified as stretching O-Sn-O (A_{1g}) and Sn-O (F_{2g}).

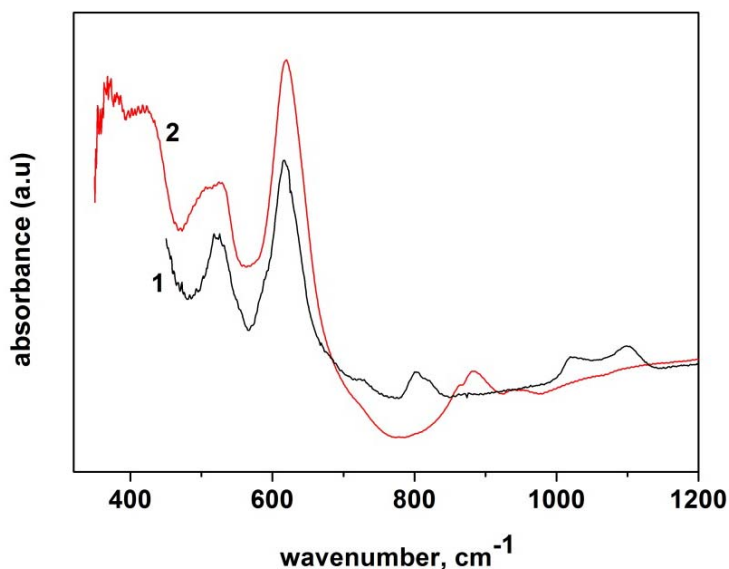


Fig. 3. IR spectra of $\text{Bi}_2(\text{Sn}_{1-x}\text{Cr}_x)_2\text{O}_7$. Curve 1 corresponds to $x = 0$, curve 2 corresponds to $x = 0.05$

Рис. 3. ИК спектры $\text{Bi}_2(\text{Sn}_{1-x}\text{Cr}_x)_2\text{O}_7$. Кривая 1 относится к $x = 0$, кривая 2 относится к $x = 0,05$

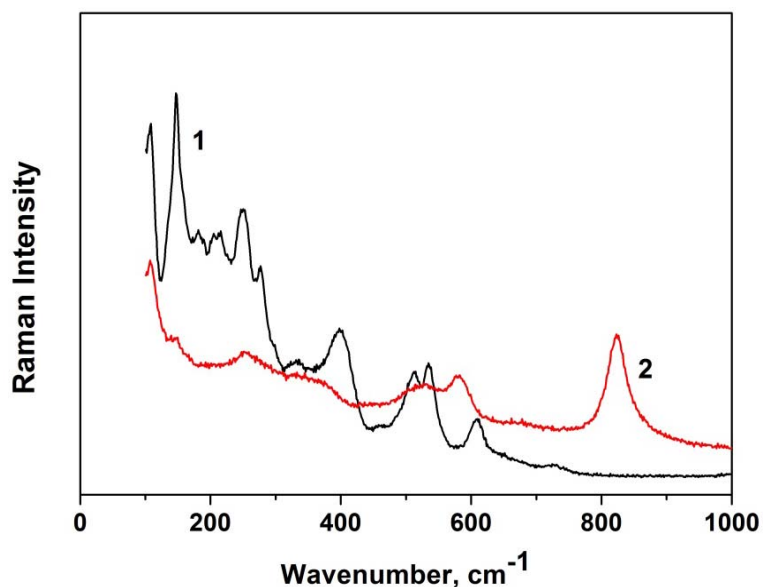


Fig. 4. Raman scattering spectrum of $\text{Bi}_2(\text{Sn}_{1-x}\text{Cr}_x)_2\text{O}_7$. Curve 1 corresponds to $x = 0$, curve 2 corresponds to $x = 0.05$

Рис. 4. Спектры Рамановского рассеяния $\text{Bi}_2(\text{Sn}_{1-x}\text{Cr}_x)_2\text{O}_7$. Кривая 1 относится к $x = 0$, кривая 2 относится к $x = 0,05$

Vibration modes of Raman and IR spectroscopy of $\text{Bi}_2(\text{Sn}_{1-x}\text{Cr}_x)_2\text{O}_7$

Raman modes (cm^{-1})		IR modes (cm^{-1})		correspondence
$X = 0$	$X = 0.1$	$X = 0$	$X = 0.05$	
108	108			A_{2u}
148	144 broad			Flexural O-Bi-O (F_{1u})
181				Bi-SnO ₆ (F_{1u})
208				
215				F_{1u}
225				F_{2g}
248	251			E_g
274				Flexural O-Sn-O (F_{1u})
332			353	F_{1u}
			382	Stretching Bi – O'
400			416 broad	Flexural O в SnO' ₆ (F_{2g})
			507	Bi-O'
512		518		Stretching SnO ₆ octahedron (A_{1g})
534	523	525	526	Flexural O' (A_{1g})
	581			Stretching Bi-O(F_{2g})
608				(F_{2g})
		615	619	Stretching Sn–O
			632	
		726		
		801		Overtone or combination
	822	820	863, 883	

The substitution of tin ions by chromium led to a decrease in the number and intensity of spectral lines of the Raman spectrum, as well as to the appearance of two new modes at frequencies of 581 and 822 cm^{-1} . The spectral line 581 cm^{-1} exists in the optical spectra of compounds with an ideal pyrochlore structure and refers to stretching vibrations of the Bi-O bond. The high-frequency spectral line 822 cm^{-1} does not have an unambiguous interpretation, and it is defined as an “overtone or combined” band (combination band) or mode (F_{2g}) [6].

Substitution of tin by Cr^{3+} ions does not change the space symmetry group and leads to the absence of some spectral lines in the spectrum of $\text{Bi}_2(\text{Sn}_{1-x}\text{Cr}_x)_2\text{O}_7$, $x = 0.1$ in comparison with $\text{Bi}_2\text{Sn}_2\text{O}_7$. Perhaps this is due to an increase in the local symmetry of bismuth pyrochlore at a disordered arrangement of Cr^{3+} ions.

Conclusion. At room temperature, bismuth pyrochlore $\text{Bi}_2(\text{Sn}_{1-x}\text{Cr}_x)_2\text{O}_7$, $x = 0; 0.05, 0.1$ refers to the monoclinic structure of *Pc*. Chromium ions replace tin ions in SnO₆ octahedra. In The IR absorption spectra four frequency regions with two absorption lines in each region, and three lines in the high-frequency region were revealed. The softening of frequencies and the type of vibration mode associated with the valence bonds of bismuth and tin at structural transitions have been established. The absence of an inversion center in doped bismuth stannates is confirmed by Raman spectra. In chromium-substituted pyrochlores, the phase boundaries of the structural transitions inherent in $\text{Bi}_2\text{Sn}_2\text{O}_7$ are shifted.

Acknowledgments. The reported study was funded by RFBR according to the research project № 20-52-00005 Bel_a.

Благодарности. Исследование выполнено при финансовой поддержке РФФИ и БРФФИ в рамках научного проекта № 20-52-00005.

References

1. Udod L. V., Aplesnin S. S., Sitnikov M. N., Molokeev M. S. Dielectric and Electrical Properties of Polymorphic Bismuth Pyrochlore $\text{Bi}_2\text{Sn}_2\text{O}_7$. *Physics of the Solid State*. 2014, Vol. 56, P. 1315–1319.
2. Udod L. V., Aplesnin S. S., Sitnikov M. N., Romanova O. B., Molokeev M. N. Phase transitions in bismuth pyrochlore upon substitution of tin by iron ions. *J. Alloys and Compounds*. 2019, Vol. 804, P. 281–287.
3. Lewis J. W., Payne J. L., Evans I. R., Stokes H. T., Branton J. Campbell and John S. O. Evans. An Exhaustive Symmetry Approach to Structure Determination: Phase Transitions in $\text{Bi}_2\text{Sn}_2\text{O}_7$. *J. Am. Chem. Soc.* 2016, Vol. 138, P. 8031–8042.
4. Udod L. V., Sitnikov M. N., Aplesnin S. S., Molokeev M. S. Electrical and Dielectric Properties of Gas-Sensor Resistive Type $\text{Bi}_2\text{Sn}_2\text{O}_7$. *Solid State Phenomena*. 2014, Vol. 215, P. 503–506.
5. Aplesnin S. S., Udod L. V., Sitnikov M. N. Electronic transition, ferroelectric and thermoelectric properties of bismuth pyrochlore $\text{Bi}_2(\text{Sn}_{0.85}\text{Cr}_{0.15})_2\text{O}_7$. *Ceramics International*. 2018, Vol. 44, P. 1614–1620.

6. Aplesnin S. S., Udod L. V., Sitnikov M. N., Kretinin V. V., Molokeev M. S., Mironova-Ulmane N. Dipole glass in chromium-substituted bismuth pyrostannate. *Mater. Res. Express*. 2018, Vol. 5, P. 115202.
 7. Aplesnin S. S., Udod L. V., Sitnikov M. N., Molokeev, M. S., Tarasova L. S., Yanushkevich K. I. Magnetic, Dielectric, and Transport Properties of Bismuth Pyrostannate $\text{Bi}_2(\text{Sn}_{0.9}\text{Mn}_{0.1})_2\text{O}_7$. *Physics of the Solid State*. 2017, Vol. 59, P. 2268–2273.
 8. Aplesnin S. S., Udod L. V., Loginov Y. Y., Kretinin V. V., Masyugin A. N. Influence of cation substitution on dielectric and electric properties of bismuth stannates $\text{Bi}_2\text{Sn}_{1.9}\text{Me}_{0.1}\text{O}_7$ (Me=Cr, Mn). *IOP Conf. Series: Materials Science and Engineering*. 2019, Vol. 467, P. 012014.
 9. Udod L. V., Aplesnin S. S., Sitnikov M. N. Magnetic Properties of Bismuth Pyrostannate Doped with 3D Ions. *Inorganic Materials: Applied Research*. 2020, Vol. 11, P. 809–814.
 10. Udod L. V., Aplesnin S. S., Sitnikov M. N., Eremin E. V., Molokeev M. S. Effect of Mn Doping on Magnetic and Dielectric Properties of $\text{Bi}_2\text{Sn}_2\text{O}_7$. *Sol. St. Phenomena*. 2015, Vol. 233–234, P. 105.
 11. Aplesnin S. S., Udod L. V., Sitnikov M. N., Eremin E. V., Molokeev M. S., Tarasova L. S., Yanushkevich K. I., Galyas A. I., Correlation of the Magnetic and Transport Properties with Polymorphic Transitions in Bismuth Pyrostannate $\text{Bi}_2(\text{Sn}_{1-x}\text{Cr}_x)_2\text{O}_7$. *Phys. Sol. St.* 2015, Vol. 57, P. 1627–1632.
 12. Aplesnin S. S., Udod L. V., Sitnikov M. N., Shestakov N. P. $\text{Bi}_2(\text{Sn}_{0.95}\text{Cr}_{0.05})_2\text{O}_7$: Structure, IR spectra, and dielectric properties. *Ceramics International*. 2016, Vol. 42, P. 5177–5183.
 13. Aplesnin S. S., Udod L. V., Sitnikov M. N., Romanova O. B. Dielectric and transport properties, electric polarization at the sequential structural phase transitions in iron-substituted bismuth pyrostannate. *Ceramics International*. 2020. Available at: <https://doi.org/10.1016/j.ceramint.2020.08.287> (accessed 25.10.2020).
 14. Udod L. V., Aplesnin S. S., Sitnikov M. N., Romanova O. B., Bayukov O. A., Vorotinov A. M., Velikanov D. A., Patrin G. S. Magnetodielectric effect and spin state of iron ions in substituted bismuth pyrostannate. *European Physical Journal Plus*. 2020. DOI: 10.1140/epjp/s13360-020-00781-2.
 15. Evans I. R., Howard J. A. K., Evans J. S. O. $\alpha\text{-Bi}_2\text{Sn}_2\text{O}_7$ – a 176 atom crystal structure from powder diffraction data. *J. Mater. Chem.* 2003, Vol. 13, P. 2098–2103.
 16. Shannon R. D. Revised effective ionic radii and systematic studies of interatomic distances in halides and chalcogenides. *Acta Cryst. A*. 1976, Vol. 32 (5), P. 751–767.
 17. Chen M., Tanner D. B., Nino J.C. Infrared study of the phonon modes in bismuth pyrochlores. *Phys. Rev. B*. 2005, Vol. 72, P. 054303-8.
 18. Moens L., Ruiz P., Delmon B., Devillers M. Cooperation effects towards partial oxidation of isobutene in multiphasic catalysts based on bismuth pyrostannate. *Appl. Catal. A: Gen.* 1998, Vol. 171, P. 131.
 19. Silva R. X., Paschoal C. W. A., Almeida R. M., M. Carvalho Castro Jr., Ayalac A. P., Auletta J. T., Lufaso M. W. Temperature-dependent Raman spectra of $\text{Bi}_2\text{Sn}_2\text{O}_7$ ceramics. *Vibrational Spectroscopy*. 2013, Vol. 64, P. 172–177.
- Библиографические ссылки**
1. Диэлектрические и электрические свойства полиморфного пиростаната висмута $\text{Bi}_2\text{Sn}_2\text{O}_7$ / Л. В. Удод, Аплеснин С. С., Ситников М. Н. и др. // Физика твердого тела. 2014. Т. 56 (7). С. 1267–1271.
 2. Phase transitions in bismuth pyrostannate upon substitution of tin by iron ions / L. V. Udod, S. S. Aplesnin, M. N. Sitnikov et. al. // J. Alloys and Compounds. 2019. Vol. 804. P. 281–287.
 3. An Exhaustive Symmetry Approach to Structure Determination: Phase Transitions in $\text{Bi}_2\text{Sn}_2\text{O}_7$ / J. W. Lewis, J. L. Payne, I. R. Evans et. al. // J. Am. Chem. Soc. 2016. Vol. 138, P. 8031–8042.
 4. Electrical and Dielectrical Properties of Gas-Sensor Resistive Type $\text{Bi}_2\text{Sn}_2\text{O}_7$ / L.V. Udod, M. N. Sitnikov, S. S. Aplesnin et. al. // Solid State Phenomena. 2014. Vol. 215. P. 503–506.
 5. Aplesnin S. S., Udod L. V., Sitnikov M. N. Electronic transition, ferroelectric and thermoelectric properties of bismuth pyrostannate $\text{Bi}_2(\text{Sn}_{0.85}\text{Cr}_{0.15})_2\text{O}_7$ // Ceramics International. 2018. Vol. 44. P. 1614–1620.
 6. Dipole glass in chromium-substituted bismuth pyrostannate / S. S. Aplesnin, L. V. Udod, M. N. Sitnikov et. al. // Mater. Res. Express. 2018. Vol. 5. P. 115202.
 7. Магнитные, диэлектрические и транспортные свойства пиростаната висмута $\text{Bi}_2(\text{Sn}_{0.9}\text{Mn}_{0.1})_2\text{O}_7$ / С. С. Аплеснин, Л. В. Удод, М. Н. Ситников и др. // Физика твердого тела. 2017. Т. 59 (11). С. 2246–2251.
 8. Influence of cation substitution on dielectric and electric properties of bismuth stannates $\text{Bi}_2\text{Sn}_{1.9}\text{Me}_{0.1}\text{O}_7$ (Me=Cr, Mn) / S. S. Aplesnin, L. V. Udod, Y. Y. Loginov et. al. // IOP Conf. Series: Materials Science and Engineering. 2019. Vol. 467. P. 012014.
 9. Udod L. V., Aplesnin S. S., Sitnikov M. N. Magnetic Properties of Bismuth Pyrostannate Doped with 3D Ions // Inorganic Materials: Applied Research. 2020. Vol. 11 (4). P. 809–814.
 10. Effect of Mn Doping on Magnetic and Dielectric Properties of $\text{Bi}_2\text{Sn}_2\text{O}_7$ / Udod L. V., S. S. Aplesnin, M. N. Sitnikov et. al. // Sol. St. Phenomena. 2015. Vol. 233–234. P. 105.
 11. Корреляция магнитных и транспортных свойств с полиморфными переходами в пиростанате висмута $\text{Bi}_2(\text{Sn}_{1-x}\text{Cr}_x)_2\text{O}_7$ / С. С. Аплеснин, Л. В. Удод, М. Н. Ситников и др. // Физика твердого тела. 2015. Т. 57 (8). С. 1590–1595.
 12. $\text{Bi}_2(\text{Sn}_{0.95}\text{Cr}_{0.05})_2\text{O}_7$: Structure, IR spectra, and dielectric properties / S. S. Aplesnin, L. V. Udod, M. N. Sitnikov et. al. // Ceramics International. 2016. Vol. 42. P. 5177–5183.
 13. Dielectric and transport properties, electric polarization at the sequential structural phase transitions in iron-substituted bismuth pyrostannate / S. S. Aplesnin, L. V. Udod, M. N. Sitnikov et. al. // Ceramics Interna-

tional. 2020 [Электронный ресурс]. URL: <https://doi.org/10.1016/j.ceramint.2020.08.287> (дата обращения: 25.10.2020).

14. Magnetodielectric Effect and Spin State of Iron Ions in Substituted Bismuth Pyrostannate / L. Udod, S. Aplesnin, M. Sitnikov et. al. // European Physical Journal Plus. 2020. DOI: 10.1140/epjp/s13360-020-00781-2.

15. Evans I. R., Howard J. A. K., Evans J. S. O. α - $\text{Bi}_2\text{Sn}_2\text{O}_7$ – a 176 atom crystal structure from powder diffraction data // J. Mater. Chem. 2003. Vol. 13. P. 2098–2103.

16. Shannon R. D. Revised effective ionic radii and systematic studies of interatomic distances in halides and chalcogenides // Acta Cryst. A, 1976. Vol. 32 (5). P. 751–767.

17. Chen M., Tanner D. B., Nino J. C. Infrared study of the phonon modes in bismuth pyrochlores // Phys. Rev. B 2005. Vol. 72. P. 054303-8.

18. Cooperation effects towards partial oxidation of isobutene in multiphasic catalysts based on bismuth pyrostannate / L. Moens, P. Ruiz, B. Delmon et. al. // Appl. Catal. A: Gen. 1998. Vol. 171. P. 131.

19. Temperature-dependent Raman spectra of $\text{Bi}_2\text{Sn}_2\text{O}_7$ ceramics / Silva R. X., C. W. A. Paschoal, R. M. Almeida, Carvalho M., Jr. Castro // Vibrational Spectroscopy. 2013. Vol. 64. P. 172–177.

© Udod L. V., Romanova O. B., Aplesnin S. S., Kretinin V. V., 2020

Udod Lubov Viktorovna – Cand. Sc., Associate Professor; Reshetnev Siberian State University of Science and Technology; Kirensky Institute of Physics, FRC KSC Siberian Branch of the Russian Academy of Sciences. E-mail: luba@iph.krasn.ru.

Romanova Oksana Borisovna – Cand. Sc., Researcher; Kirensky Institute of Physics, FRC KSC Siberian Branch of the Russian Academy of Sciences. E-mail: rob@iph.krasn.ru.

Aplesnin Sergey Stepanovich – Dr. Sc., Professor, Head of the Department of Physics; Reshetnev Siberian State University of Science and Technology; Kirensky Institute of Physics, FRC KSC Siberian Branch of the Russian Academy of Sciences. E-mail: aplesnin@sibsau.ru.

Kretinin Vasily Vasilievich – student of the Department of Physics; Reshetnev Siberian State University of Science and Technology. E-mail: kretinin.vasya@yandex.ru.

Удод Любовь Викторовна – кандидат физико-математических наук, доцент; Сибирский государственный университет науки и технологий имени академика М. Ф. Решетнева; Институт физики им. Л. В. Киренского СО РАН – обособленное подразделение ФИЦ КИЦ СО РАН. E-mail: luba@iph.krasn.ru.

Романова Оксана Борисовна – кандидат физико-математических наук, научный сотрудник; Институт физики им. Л. В. Киренского СО РАН – обособленное подразделение ФИЦ КИЦ СО РАН. E-mail: rob@iph.krasn.ru.

Аплеснин Сергей Степанович – доктор физико-математических наук, профессор, заведующий кафедрой физики; Сибирский государственный университет науки и технологий имени академика М. Ф. Решетнева; Институт физики им. Л. В. Киренского СО РАН – обособленное подразделение ФИЦ КИЦ СО РАН. E-mail: aplesnin@sibsau.ru, apl@iph.krasn.ru.

Кретинин Василий Васильевич – студент; Сибирский государственный университет науки и технологий имени академика М. Ф. Решетнева. E-mail: kretinin.vasya@yandex.ru.
